

Influence of low ambient pressure on the performance of a high-energy array surface arc plasma actuator

Bing-Liang Tang(唐冰亮), Shan-Guang Guo(郭善广), Hua Liang(梁华), Meng-Xiao Tang(唐孟潇)

Citation: Chin. Phys. B . 2020, 29(10): 105204 . **doi:** 10.1088/1674-1056/aba9c8
Journal homepage: http://cpb.iphy.ac.cn; http://iopscience.iop.org/cpb

What follows is a list of articles you may be interested in

Discharge simulation and volt-second consumption analysis during ramp-up on the CFETR tokamak

Cheng-Yue Liu(刘成岳), Bin Wu(吴斌), Jin-Ping Qian(钱金平), Guo-Qiang Li(李国强), Ya-Wei Hou(侯雅巍), Wei Wei(韦维), Mei-Xia Chen(陈美霞), Ming-Zhun Lei(雷明准), Yong Guo(郭勇)

Chin. Phys. B . 2020, 29(2): 025202 . **doi:** 10.1088/1674-1056/ab610d

Analytical studies on the evolution processes of rarefied deuterium plasma shell Z-pinch by PIC and MHD simulations

Cheng Ning(宁成), Xiao-Qiang Zhang(张小强), Yang Zhang(张扬), Shun-Kai Sun(孙顺凯), Chuang Xue(薛创), Zhi-Xing Feng(丰志兴), Bai-Wen Li(李百文)

Chin. Phys. B . 2018, 27(2): 025207 . **doi:** 10.1088/1674-1056/27/2/025207

Modeling and optimization of the multichannel spark discharge

Zhi-Bo Zhang(张志波), Yun Wu(吴云), Min Jia(贾敏), Hui-Min Song(宋慧敏), Zheng-Zhong Sun(孙正中), Ying-Hong Li(李应红)

Chin. Phys. B . 2017, 26(6): 065204 . **doi:** 10.1088/1674-1056/26/6/065204

End-on x-ray backlighting experiments for axial diagnostics of wire-array Z-pinch plasma on PPG-1

Shen Zhao(赵屾), Xinlei Zhu(朱鑫磊), Huantong Shi(石桓通), Xiaobing Zou(邹晓兵), Xinxin Wang(王新新)

Chin. Phys. B . 2017, 26(1): 015206 . **doi:** 10.1088/1674-1056/26/1/015206

Fabricating a reactive surface on the fibroin film by a room-temperature plasma jet array for biomolecule immobilization

Chen Guang-Liang, Zheng Xu, Lü Guo-Hua, Zhang Zhao-Xia, Sylvain Massey, Wilson Smith, Michael Tatoulian, Yang Si-Ze

Chin. Phys. B . 2012, 21(10): 105201 . **doi:** 10.1088/1674-1056/21/10/105201

Influence of low ambient pressure on the performance of a high-energy array surface arc plasma actuator

Bing-Liang Tang(唐冰亮), Shan-Guang Guo(郭善广), Hua Liang(梁华)†, and Meng-Xiao Tang(唐孟潇)

Science and Technology on Plasma Dynamics Laboratory, Air Force Engineering University, Xi'an 710038, *China*

(Received 26 May 2020; revised manuscript received 11 July 2020; accepted manuscript online 28 July 2020)

In order to solve the problem of single arc plasma actuator's failure to suppress the boundary layer separation, the effectiveness of the array surface arc plasma actuator to enhance the excitation intensity is verified by experiment. In this study, an electrical parameter measurement system and high-speed schlieren technology were adopted to delve into the electrical, flow field, and excitation characteristics of the high-energy array surface arc plasma actuator under low ambient pressure. The high-energy array surface arc discharge released considerable heat rapidly; as a result, two characteristic structures were generated, i.e., the precursor shock wave and thermal deposition area. The duration increased with the increase in environmental pressure. The lower the pressure, the wider the thermal deposition area's influence range. The precursor shock wave exhibited a higher propagation speed at the initial phase of discharge; it tended to decay over time and finally remained at 340 m/s. The lower the environmental pressure, the higher the speed would be at the initial phase. High-energy array surface arc plasma actuator can be employed to achieve effective high-speed aircraft flow control.

Keywords: low ambient pressure, high-energy, array, surface arc plasma actuator

PACS: 52.50.−b, 52.35.Ra, 52.30.−q, 52.50.Gj **DOI:** 10.1088/1674-1056/aba9c8

1. Introduction

As fueled by the advancement of aerospace technology and advanced engine technology, high-speed aircraft is subject to increasingly sophisticated flow problems.[1,2] Thus, novel control technologies should be explored to enhance the flight control performance of high-speed aircraft.[3,4] Effective flow control methods can be divided into passive control and active control.[5] Besides, the active control technology is capable of modifying the control strategy in real time abiding by the working state of the controlled object; it also exhibits flexible layout, thereby avoiding the mutual interference between the actuator and the flow field, as well as additional resistance.[6,7] It has been extensively adopted to inhibit flow separation,[8] boundary layer transition,[9] and drag reduction.[10]

Plasma flow control refers to an active flow control technology complying with the emerging concept of plasma aerodynamic excitation. Given a variety of action forms, typical plasma actuators include dielectric barrier discharge plasma actuators, plasma synthesis jet actuators, and surface arc plasma actuators. The dielectric barrier discharge actuator exhibits relatively weak disturbance intensity; besides, the flow control effect is difficult to enhance, which is not suitable for high-speed flow control.[11] Pulsed arc discharge plasma actuators and plasma synthetic jet actuators have been primarily discussed in most studies on supersonic flow control worldwide. The plasma synthetic jet exhibits a large excitation intensity, whereas under the physical limitations of the cavity, a saturation frequency is identified. The need of supersonic flow for high frequency excitation is difficult to satisfy.[12] The surface arc plasma actuator exhibits more advantages in supersonic flow control. Moreover, the technical advantages have been elucidated. First, the excitation intensity is large, so shock waves can be generated to satisfy the high-intensity excitation requirements. Second, the electrode is flush with the wall surface, and no additional resistance is identified.

The surface arc plasma actuator, as an emerging active flow control technology, has promising applications in high-speed aircraft flow control for its simple structure, large excitation intensity, and fast response.[13] Samimy *et al.* in 2004 initially proposed the concept, which was introduced to control compressible jets. Because of the large excitation intensity, it has been progressively applied in high-speed flow control research.[14] Bletzinger drew the general control principle of pulsed arc discharge in his review. The energy deposition in the excitation zone can enhance the local sound velocity and down-regulate the Mach number, so the control effect can be achieved, i.e., the flow field is modified.[15]

The existing surface arc plasma excitation employed for the flow control of high-speed aircraft is formed as a pulse arc. With the increase in the excitation frequency, the control time of the plasma excitation is prolonged. Samimy's team experimentally studied controlling shock wave boundary layer interaction by pulsed arc plasma excitation. To be specific, a group of actuators were arranged in the upstream of the shockwave, and the excitation frequency was in kHz. Shock instability decreased, whereas the frequency of instability remained unchanged, and the separation was not suppressed.[16,17] As revealed from the analysis, the main cause of the poor flow control effect is due to insufficient ex-

†Corresponding author. E-mail: lianghua82702@126.com

© 2020 Chinese Physical Society and IOP Publishing Ltd

citation intensity and frequency, so a stable control effect is difficult to form.[18–20] To develop an effective way of stability control, the present study proposed adopting a large energy array surface arc plasma actuator control mode to enhance the excitation intensity and prolong the duration to satisfy the requirements of high-intensity large-area excitation.

The studies on the characteristics of surface arc plasma discharge worldwide highlight two aspects, i.e., the structural parameters (e.g., electrode spacing and size), and the discharge parameters (e.g., excitation voltage and capacitance).[20–24] One of the critical factors, the working ambient pressure, however, is often overlooked.[25–28] In existing studies, the working ambient pressure as a critical parameter affecting the performance of the surface arc plasma actuator has not been quantitatively explored. Since the pressure of supersonic incoming conditions is associated with the Mach number, the higher the Mach number is, the lower the local static pressure will be. For the discharge, the lower the ambient pressure is, the easier a discharge will be formed, whereas the energy deposited by the arc discharge into the air is lowered. Accordingly, the ambient pressure significantly impacts the surface arc discharge characteristics.[29–33] Moreover, the response of the perturbation effect exerted by the arc discharge to different pressures is critical to optimize the actuator performance. The performance of surface arc actuators under low ambient pressure requires further determination.

To satisfy the critical requirements of plasma flow control for the novel generation of supersonic or hypersonic aircraft, the discharge and flow field evolution characteristics of the high-energy array surface arc plasma actuator under low ambient pressure static state were studied with the electrical parameter measurement and high-speed schlieren systems. Furthermore, the present study delved into the effects of ambient pressure and DC voltage on the duration of the thermal deposition and the propagation velocity of the shock wave.

2. Experiment set-up

2.1. Discharge circuit and schlieren system

To generate a robust discharge between the electrodes, an external circuit was connected in parallel to a microsecond pulsed power supply with a peak voltage of 20 kV and pulse duration of 2 μs. The external circuit consisted of a high-voltage DC power supply with an output voltage ranging from 0 to 10 kV, as well as a capacitance of 10 μF. The high-voltage pulsed circuit induced the gas breakdown, lasting for nearly 1 μs. The second step was the energy deposition from the capacitor to the discharge channel, lasting for a few microseconds.

In this study, a schlieren system was employed for flow visualization and measurement; with this system, the flow field could be characterized distinctly from the variation in the grey values. A continuous, high-power, bi-xenon head lamp acted as the light source; via convex lenses, the light was converged to a point. The light path led to the formation of a "Z" shape (Fig. 1). In the experiment, the exposure time of the high-speed camera reached 1 μs, and the frame frequency was 5000 Hz, so the frame interval was 20 μs. The size of each image is 512×512 pixels. To ensure unity, the camera parameters were kept unchanged in all experiments.

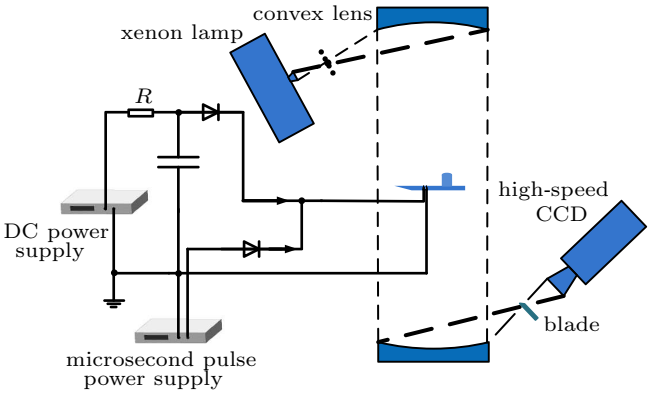


Fig. 1. Schematic diagram of discharge circuit and schlieren system.

2.2. Actuator layout

Figure 2 illustrates the structural layout of the array excitation. The design size of the acrylic plate was 400 mm $(L) \times 110$ mm (W). The cylindrical protrusion exhibiting a height of 20 mm acted as a vertical calibration to determine the distance traveled by the shock wave, as an attempt to calculate the propagation speed of the shock wave. The cylindrical protrusion was fixed at the rear edge of the plate. The leading edge was 285 mm. The first set of arc actuator was 215 mm away from the leading edge, and three sets of arc actuators were installed along the center of the flat plate, with a distance of 30 mm between each other and an electrode spacing of 5 mm. The arc actuator was simple in structure and consisted of a teflon cylinder and a copper needle (1 mm), as embedded on the plate surface. The discharge circuit was designed in series, and the three groups of electrodes were connected in series in sequence. The left-end electrode was linked to the input end of the discharge circuit, the electrode at the right end was grounded, and the middle electrode was connected in sequence.

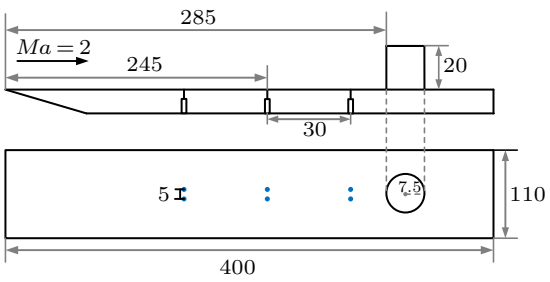


Fig. 2. Schematic diagram of actuator layout (unit: mm).

2.3. Electrical parameters of the test system

Under the discharged actuator, a highvoltage probe (P6015A, Tektronix) linked to the highvoltage end of the electrode was adopted to determine the discharge voltage waveform. A current loop (Pearson 6600) was adopted to measure the discharge current waveform. The resulting voltage and current data were recorded on an oscilloscope (DPO4104, Tektronix) under a sampling frequency of 1 GHz. The variation of the instantaneous power of the discharge over time could be expressed as $P(t) = U(t) \cdot I(t)$. The energy in a single pulse discharge could be calculated by integrating the instantaneous power over time $E_C = \int_0^t p(t)\,\mathrm{d}t$.

3. Results and discussion

3.1. Discharge characteristics

Figure 3(a) presents the voltage and current evolution of the high-energy array surface arc actuator instantaneous discharge. The environmental pressure was 20 kPa. The DC voltage was 4 kV. As suggested by this figure, under low pressure, the breakdown voltage of the arc discharge was up to 4.5 kV, the discharge current reached 1.5 kA, and the time scale of discharge was nearly 45 μs. The variation in voltage complied with the process of breakdown arcing, and the energy deposition after breakdown was consistent with the change of the current. Figure 3(b) presents a waveform diagram of the discharge power $P(t)$ calculated from the voltage and current data. The single discharge energy E_c could be determined by integrating it with time as 36.9 J, and the overall discharge energy could be defined as the energy initially stored in the capacitor $E_0 = 1/2CU_{DC}^2$. The energy stored in the capacitor was 80 J. The discharge energy conversion rate $\eta_0 = E_c/E_0 = 46\%$.

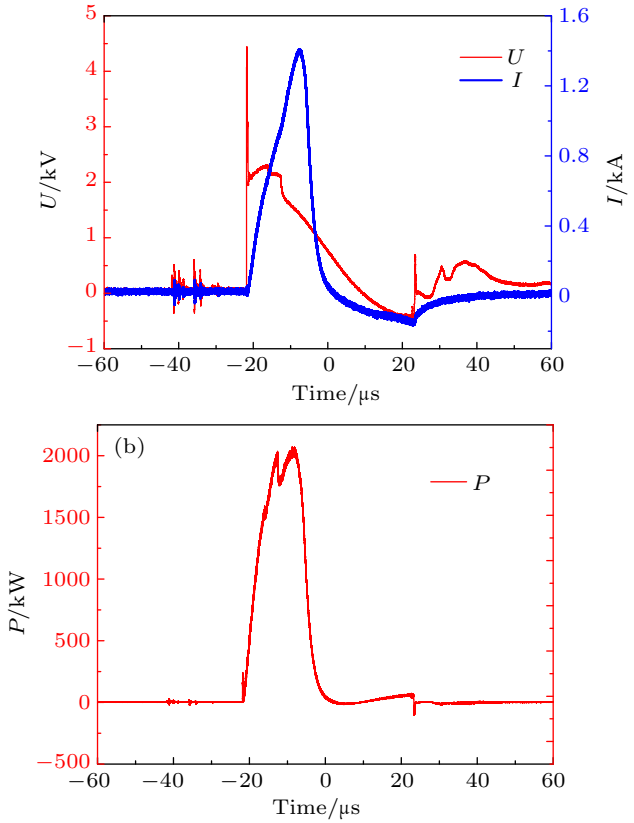


Fig. 3. Discharge characteristics: (a) voltage–current waveform, (b) power waveform.

Figure 4 presents the discharge voltage and current waveform under the changed DC voltage. As suggested by this figure, under the DC voltage of 1 kV, the breakdown voltage that forms the arc discharge was 3.1 kV, the discharge current was 16 A, and the time scale of discharge was about 40 μs. The breakdown voltage and discharge current between the electrodes were positively related to the DC voltage. With the rise of the DC voltage, the capacitor was charged with more charge, so a single pulse could release more energy and corresponding more power. It is therefore revealed that the DC voltage is one of the main circuit parameters determining the strength of the actuator.

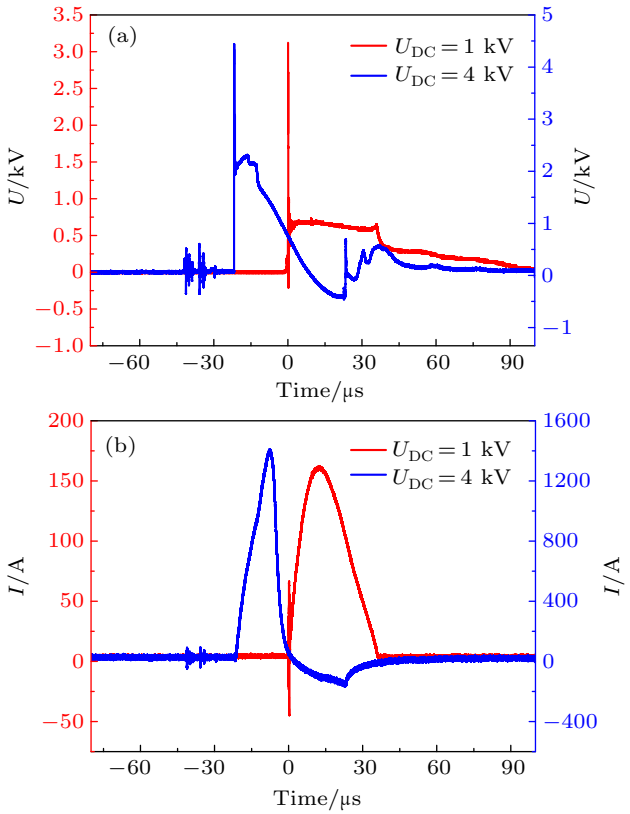


Fig. 4. Discharge waveforms at different DC voltages: (a) voltage waveform, (b) current waveform.

3.2. Typical flow field evolution

To analyze the flow field structure generated by the high-energy array surface arc excitation under the low ambient pres-

sure, the ambient pressure was set at 20 kPa, and the DC voltage was set at 4 kV. Figure 5 illustrates the flow field evolution structure of the three groups of actuators. At $t = 40$ μs, the precursor shock waves generated by the three sets of actuators simultaneously formed a precursor shock wave train, propagating upward at the identical diffusion speed. The precursor shock waves interfered with each other to develop a complex wave system. At $t = 1080$ μs, the thermal deposition area began to diffuse, and the squeeze vortex structure was formed as impacted by the interaction between the two adjacent thermal deposition areas. Moreover, the internal structure of the thermal deposition area began to fall off and float upward. After 3600 μs, the bottom layer of the thermal deposition area began to dissipate into a small-scale vortex structure, and the deposition area began to display a slow growth. Accordingly, the area affected by the arc discharge could be determined.

Figure 5 suggests that surface arc discharge released considerable heat rapidly and formed two characteristic structures, i.e., a precursor shock wave and a thermal deposition area. The precursor shock wave was generated by sudden temperature rise, and thermal expansion of the gas. The shock wave exhibited a fast speed and a large instantaneous thrust. The main shock effect was generated by the flow field. The arc that was heating the local air generated the thermal deposition area and carried considerable heat. It lasted for a long time and spreaded around over time. The disturbance area was large, and the thermal effect was applied to the boundary layer of the flow field. The propagation speed of the shockwave formed by arc discharge was fast, and its evolution soon went beyond the observation range of the existing field of view. The thermal deposition area formed by arc discharge was free to spread around without directivity. As compared with a plasma synthetic jet actuator, the high-energy array surface arc actuator was capable of maximizing the energy release. As suggested from the above analysis, the surface arc plasma excitation that adopted an array layout and high-energy discharge exerted an effect on the whole area.

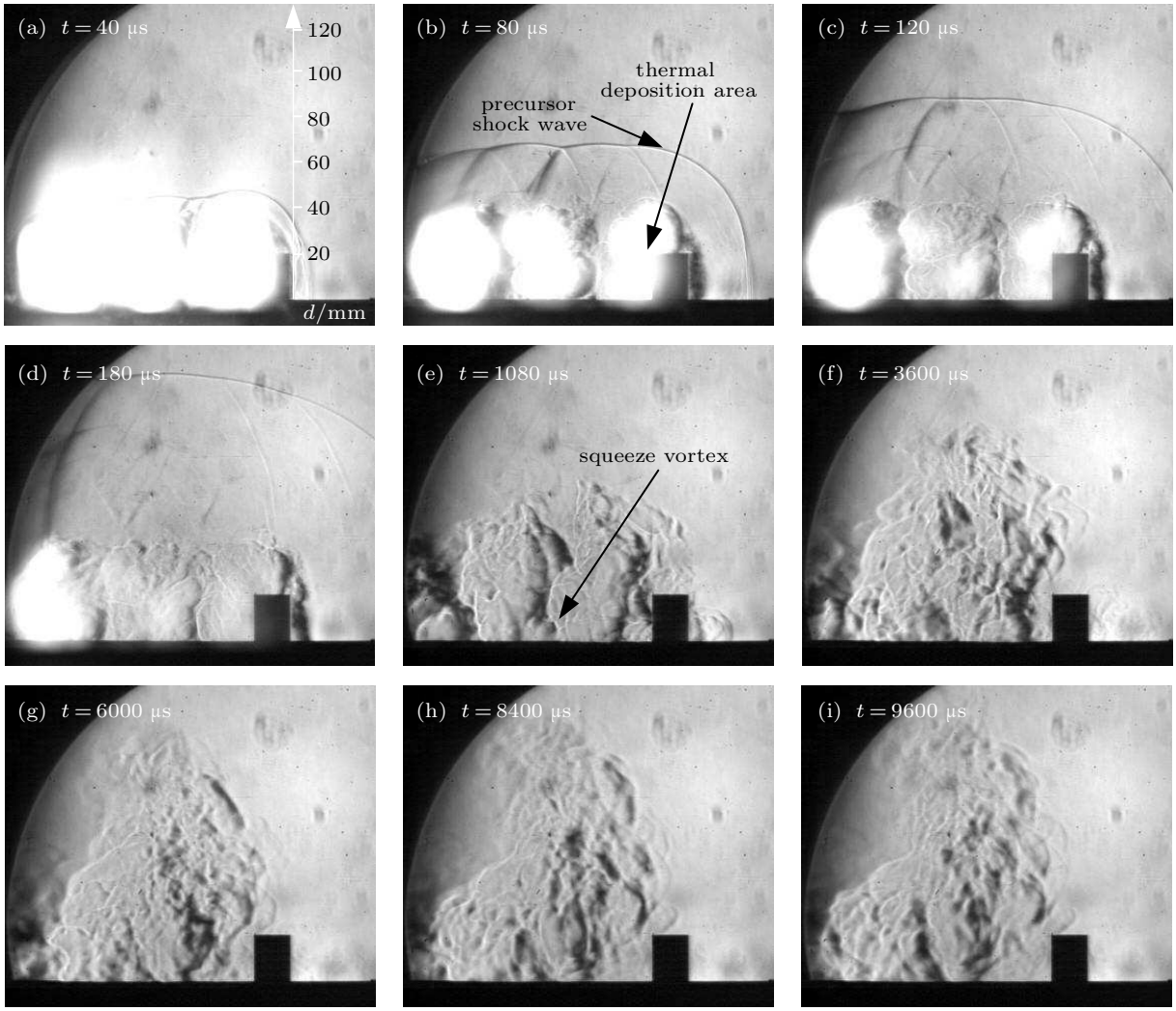


Fig. 5. Flow field evolution.

To delve into the characteristics of the thermal deposition area, an image processing method was introduced to obtain the duration of the thermal deposition area. In brief, a rectangular monitoring matrix was set in view (the coverage of the monitoring matrix selected in the present study was 242×272). When there was no discharge, the gray value matrix of the monitoring matrix was $A_{242\times272}$. After applying the discharge, the gray value matrix of the monitoring matrix was $B_{242\times272}$. Through the mentioned two parameters, the average gray value difference in the monitoring area could be expressed as

$$Q = \frac{1}{242 \times 272} \sum_{j=1}^{272} \sum_{i=1}^{242} \left| B_{ij} - A_{ij} \right|,$$

where Q denotes a comprehensive evaluation parameter that can reflect both the duration of the thermal deposition zone and its deposition energy intensity. The larger the difference is, the more obvious the variation would be in the monitoring area. The larger corresponding deposition energy and the change curve of Q over time could be exploited to obtain the duration of the thermal deposition zone. In Fig. 6, the blue rectangular frame in the figure represents the monitoring area. The change curve of the Q value is suggested to be stepwise. Before 440 μs, the thermal deposition area was hemispherical and close to the wall surface, so it maintained a high intensity in the monitoring area. Subsequently, the average gray-scale difference value decreased to nearly 14 and remained stable, revealing that the monitoring area was stably covered by thermal deposition. The second sudden variation in the monitored Q value occurred at about 3600 μs, demonstrating that the thermal deposition in the monitored area began to weaken. After 6600 μs, the average gray value difference became stable again and maintained at a low level, revealing no significantly thermal deposition within the monitoring area at this time. As revealed from the results, the thermal deposition effect in the monitoring area was obvious before the average gray value difference Q decreased for the second time. Thus, the critical state of the thermal deposition zone phenomenon was set to 50% of the second falling edge. Under this discharge condition, the duration of the deposition energy characteristic was 4200 μs.

Figure 7 presents the evolution of the flow field structure under different pressure conditions (6 kPa, 10 kPa, 20 kPa, 50 kPa) at different time (40 μs, 440 μs, 1080 μs, 1680 μs). The DC voltage was 4 kV. At $t = 40$ μs, the size of the thermal deposition zone was close under different pressures. Though the size was not significantly different, the energy deposited in the air increased with the rise in the pressure. Moreover, the strength of the shock wave was weak under low pressure. After discharge, the thermal deposition area tended to float slightly upward for its small density. By comparing the schlieren images under different ambient pressures, the thermal deposition area produced under the 6 kPa ambient pressure was dark, and the outline was unclear. The main reason was that the energy deposition should have a medium. The lower the ambient pressure, the lower the gas density would be. The corresponding medium for absorbing energy was reduced, so the energy deposition appeared to decrease. Under high pressure, significant turbulent and vortex structures were generated in the thermal deposition area, and the boundary contour was clearer.

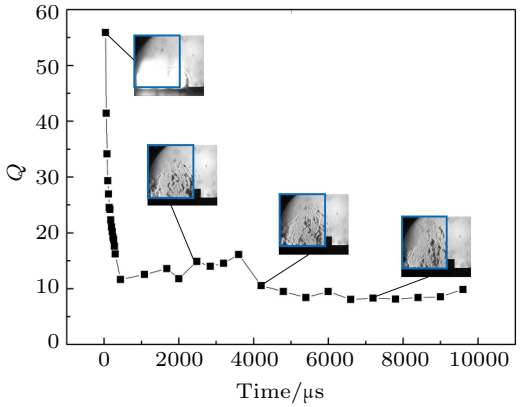


Fig. 6. Difference of mean gray value in monitoring area.

The mentioned results were caused by two reasons. First, the pressure was high, the density was high, and the intensity of the discharge was greater. The generated deposition energy was easy to cause shear dissipation in the deposition area to form a turbulent structure. The second reason was the deposition area and the surrounding gas. Shearing was easy to occur, and vortices were formed. With the decrease in ambient pressure, the shear dissipation decreased, and the thermal deposition zone gradually exhibited a laminar flow state. Under low ambient pressure, the energy deposition in the thermal deposition zone was faster. At 6 kPa, the thermal deposition zone almost disappeared after 1080 μs. According to the above analysis, the size of the thermal deposition area was sensitive to the pressure, and the deposition energy generated by the surface arc discharge was positively related to the pressure.

Figure 8 illustrates the evolution of the flow field structure at different DC voltages U_{DC}. The ambient pressure was 20 kPa, and the DC voltage was 1 kV or 4 kV. The shock wave became more robust with the elevation of the DC voltage. Since the ambient pressure was low, the shock wave decreased rapidly. The thermal deposition zone turned more robust with the rise of the DC voltage. With the rise of the DC voltage, squeeze vortices started to appear between two adjacent actuators, demonstrating that free shear started to occur within the thermal deposition zone, and energy began to dissipate. The discharge characteristics of Fig. 4 are further intuitively presented in the schlieren image. The elevation of DC voltage was conducive to enhancing the excitation effect.

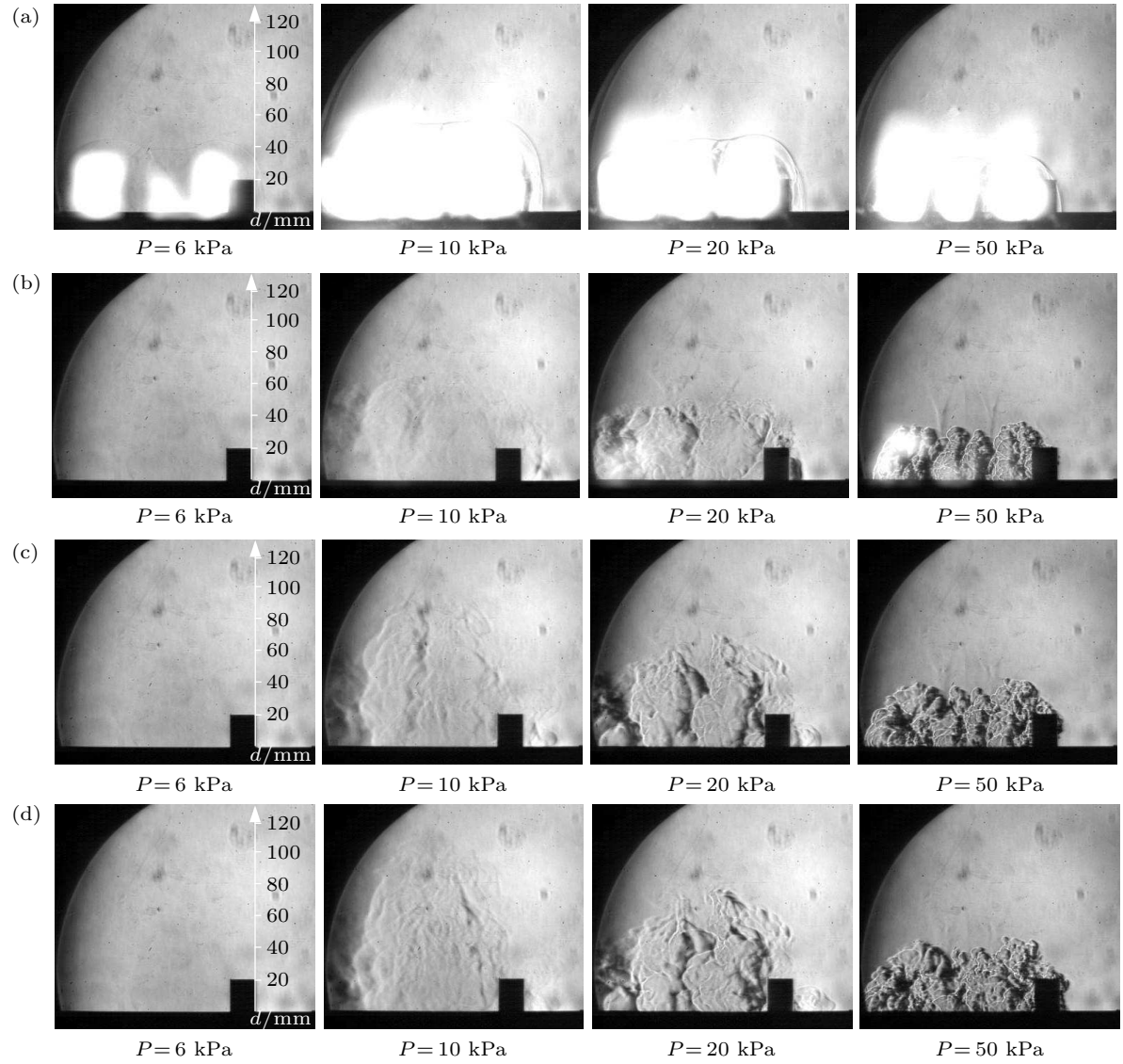


Fig. 7. The flow field structure of arc discharge under different pressure: (a) $t = 40$ μs, (b) $t = 440$ μs, (c) $t = 1080$ μs, (d) $t = 1680$ μs.

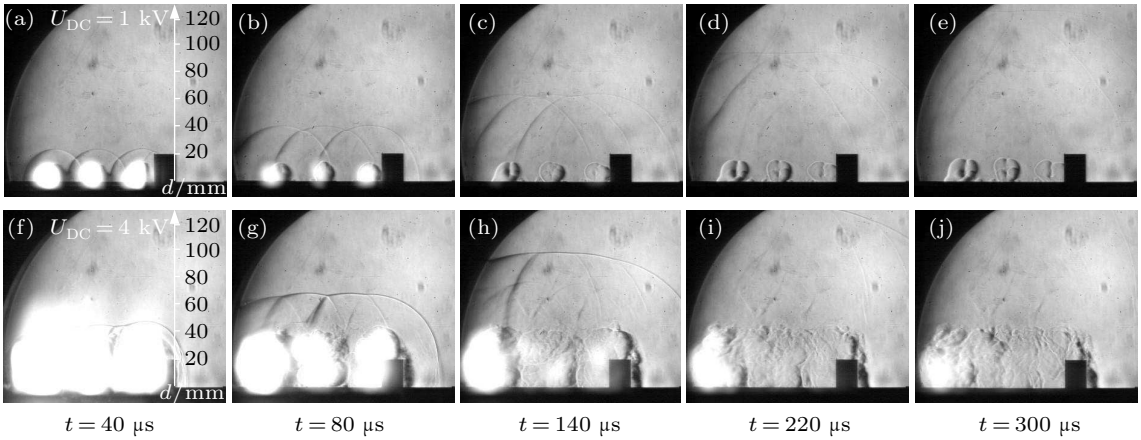


Fig. 8. The flow field structure for different DC voltage under ambient pressure of 20 kPa.

3.3. Characteristic research

The thermal deposition zone characterized the feasibility of surface arc actuators, suggesting that the control effect of the actuator in the supersonic flow field was usually determined by the influence range of the thermal deposition area after the excitation was applied. According to the calculation method of the duration of the thermal deposition zone defined above, the duration of the thermal deposition zone under dif-

ferent pressure conditions was calculated (Fig. 9). Under the DC voltage of 4 kV, the duration of the thermal deposition zone was significantly longer than that under the DC voltage of 1 kV. According to the voltage-current curve (Fig. 4), the larger the charging voltage, the more the energy would be released by the discharge; therefore, the longer the duration of the thermal deposition zone. The duration extended slowly with the reduction of the ambient pressure. As the pressure further increased, the duration was extended linearly and sharply. As revealed from the analysis, the duration of the thermal deposition zone was extremely sensitive to pressure changes. The higher the pressure, the greater the gas density would be. As a result, more ions were released to support the discharge, which enhanced the intensity and extended the duration.

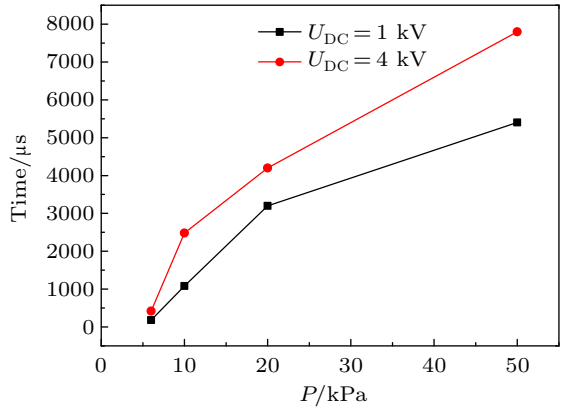


Fig. 9. The variation of thermal deposition with pressure.

To delve into the effect of ambient pressure and DC voltage via the frame frequency of a high-speed camera and the position of the precursor shock wave at different instantaneous cross-sections, this study determined the head propagation velocity of the precursor shockwave in a range of time (Fig. 10). Initially, the shock wave exhibited a fast propagation speed, whereas it gradually decreased over time. Under the DC voltage of 4 kV, the propagation velocity of the shockwave was significantly higher than that under the DC voltage of 1 kV. Combined with the voltage and current curve (Fig. 4), the higher the charging voltage, the more energy was released during the discharge, and the faster the propagation velocity of the shockwave. Under the DC voltage of 4 kV, no matter how the ambient pressure changed, at 120 μs, the propagation speed was close to 340 m/s. Under the DC voltage of 1 kV, no matter how the ambient pressure changed, at 100 μs, the propagation speed was close to 340 m/s. Likewise, by combining with the voltage and current curve (Fig. 4), the higher the charging voltage, the more the energy would be released from the discharge, and the longer the discharge time would be, so the propagation velocity of the shock wave decreased more slowly.

The shock wave induced by the arc discharge under low ambient pressure exhibited higher initial propagation velocity, and its velocity attenuation was sharp as well. Compared with existing studies,[33] the shockwave obtained in the present study propagated faster, demonstrating that the shock wave was more robust. To disturb the supersonic flow field, a certain impact effect should be exerted first. The high-energy surface arc array excitation exhibited a robust shock wave strength under low pressure, revealing that it will also have a strong control ability for the supersonic flow field.

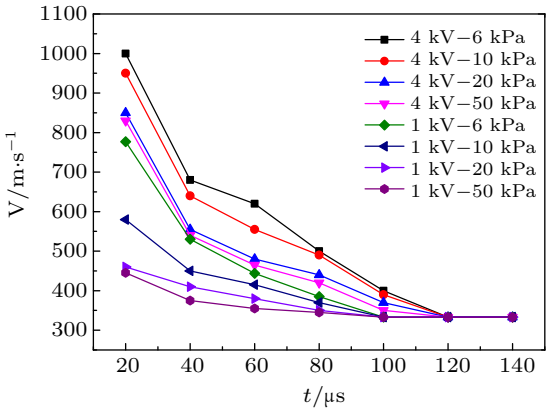


Fig. 10. The velocity of a shockwave under different pressures.

4. Conclusion

The electrical parameter test system and high-speed schlieren system were used to study the characteristics of the high-energy array surface arc actuator under low ambient pressure. The effect of ambient pressure and DC voltage on the discharge characteristics and excitation effect was obtained. The effect of ambient pressure and DC voltage on the duration of thermal deposition area and the speed of shock wave propagation was also obtained. The present study validates the feasibility of the high-energy array surface arc actuator as an active flow control device for high-speed aircraft, and provides parameter selection for the high-energy array surface arc exciter to achieve active flow control of supersonic flow field. The main conclusions are drawn as follows.

(I) When the ambient pressure was 20 kPa and the DC voltage was 4 kV, the breakdown voltage of the arc discharge was up to 4.5 kV, the discharge current reached 1.5 kA, and the time scale of the discharge was about 45 μs. Using the external circuit in this article can improve the discharge current. The longer duration of the current was the main cause of energy deposition. The breakdown voltage and discharge current between the electrodes were positively related to the DC voltage. The DC voltage was one of the main circuit parameters determining the strength of the actuator.

(II) A single discharge induces two structural characteristics in the flow field, i.e., a precursor shock wave and a thermal deposition area. The shock wave propagation speed decays over time. The larger the DC voltage, the slower the shock wave propagation speed decays. The shock wave exhibited a

fast propagation speed at the initial phase, gradually decayed over time, and finally remained at 340 m/s. The lower the ambient pressure, the higher the speed would be at the initial phase. When the ambient pressure was 6 kPa and the DC voltage was 4 kV, the maximum shock wave speed was 1020 m/s. Under low ambient pressure, the high-energy array surface arc excitation exhibited a strong shock wave intensity, demonstrating that it would exhibit robust control ability in the supersonic flow field.

(III) Ambient pressure significantly impacted the excitation characteristics, especially under low ambient pressure. The lower the ambient pressure, the faster the thermal deposition zone would decay. Moreover, the thermal deposition zone duration was shortened with the reduction of ambient pressure. Regardless of the variation of ambient pressure, a maximum impact range was identified in the thermal deposition zone, hardly varying with the variation of ambient pressure.

(IV) The duration of the thermal deposition area was prolonged with the rise of the environmental pressure, and it grew slowly with the reduction of the ambient pressure. The duration was 4200 μs, and it increased sharply in a linear trend. The greater the DC voltage, the longer the duration of the thermal deposition zone would be extended.

References

[1] Curran E T 2001 *J. Propul. Power* **17** 1138
[2] Liu X H, Lai G W and Wu J 2018 *Acta Aerodyn. Sin.* **36** 196 (in Chinese)
[3] Zhang Z X, Wu Y H and Chu W L 2010 *J. Aero. Power.* **25** 1615 (in Chinese)
[4] Sonoda T, Arima T, Olhofer M, Sendhoff B and Kost F 2004 *J. Turbomach* **128** 1275
[5] Küchemann 1965 *Prog. Aeronaut. Sci.* **6** 271
[6] Dolling D S 2001 *AIAA J.* **39** 1517
[7] Zheltovodov A A and Pimonov E A 2013 *Tech. Phys.* **58** 170
[8] Selig M S and Smits A J 2016 *AIAA J* **29** 1651
[9] Schulein E and Zheltovodov A A 2011 *Shock Waves* **21** 383
[10] Zheltovodov A A, Pimonov E A and Knight D 2007 *Shock Waves* **17** 273
[11] Li, J F and Zhang X B 2020 *J. Phys. D: Appl. Phys.* **53** 235204
[12] Kozato Y, Kikuchi S, Imao S, Kato Y and Okayama K 2016 *Int. J. Heat Fluid Flow* **62** 33
[13] Hahn C, Kearney-Fischer M and Samimy M 2011 *Exp. Fluids* **51** 1591
[14] Samimy M, Adamovich I and Webb B 2004 *Exp. Fluids* **37** 577
[15] Bletzinger P and Ganguly B N 2005 *J. Phys. D: Appl. Phys.* **38** 33
[16] Webb N, Clifford C and Samimy M 2011 41*st AIAA Fluid Dynamics Conference and Exhibit*, June 27–30,2011, Hawaii, USA, p. 3273
[17] Webb N, Clifford C and Samimy M 2011 41*st AIAA Fluid Dynamics Conference and Exhibit*, June 27–30, 2011, Hawaii, USA, p. 3426
[18] Balcon N, Benard N and Braud P 2008 *J. Phys. D: Appl. Phys.* **41** 205204
[19] Pafford B, Sirohi J and Raja L L 2013 *J. Phys. D: Appl. Phys.* **46** 485208
[20] Hahn C, Kearney-Fischer M and Samimy M 2011 *Exp. Fluids* **51** 1591
[21] Sinha A, Alkandry H and Kearney-Fischer M 2012 *Phys. Fluids* **24** 125104
[22] Kleinman B B, Bodony D J and Freund J B 2010 *Phys. Fluids* **22** 305
[23] Leonov S B and Yarantsev D A 2008 *J. Propul. Power* **24** 1168
[24] Gaitonde D V 2013 *Comput. Fluids* **85** 19
[25] Glumac N and Elliott G 2007 *Opt. Lasers Eng.* **45** 27
[26] Liu J H 2014 *Investigations of Pulse Discharge Propagation under Varying Gas Pressure* (Ph.D. Dissertation) (WuHan: Huazhong University of Science and Technology) (in Chinese)
[27] Wang Q 2018 *Study on The Effect of Plasma Discharge Enhancement in Low Pressure Plasma* (MS dissertation) (BeiJing: Beijing University Of Technology) (in Chinese)
[28] Cao X 2015 *Investigation of Pulse Discharge under Low Air Pressure* (Ph.D.Dissertation) (WuHan: Huazhong University of Science and Technology) (in Chinese)
[29] Gan T, Wu Y, Sun Z Z, Jin D, Song H M and Jia M 2018 *Phys. Fluids* **30** 055107
[30] Sun Q, Cui W, Li Y H, Cheng B Q, Jin D and Li J 2014 *Chin. Phys. B* **23** 075210
[31] Sun Q, Li Y, Cheng B, Cui W, Liu W and Xiao Q 2014 *Phys. Lett. A* **378** 2672
[32] Zong H H, Cui W, Wu Y, Zhang Z B, Liang H, Jia M and Li Y H 2015 *Sens. Actuator A-Phys.* **222** 114
[33] Gan T, Jin D, Guo S and Wu Y 2018 *Contrib. Plasma Phys.* **58** 260